

Jin et al., <http://www.jgp.org/cgi/content/full/jgp.201210883/DC1>

Table S1 provides the discretized equivalents of the differential and integration equations used in the model formulation (Table 1).

#### Discretization method

The diffusion equation was solved numerically by the Crank-Nicolson method using spatial discretization (second-order central difference scheme). Diffusion in astrocyte cytoplasm was computed using the one-dimensional diffusion equation,

$$\frac{dc}{dt} = \frac{d}{dx} \left( D \frac{dc}{dx} \right) = \frac{dD}{dx} \frac{dc}{dx} + D \frac{d^2c}{dx^2}, \quad (\text{S1})$$

where D is diffusion coefficient, c is the concentration of K<sup>+</sup> or non-K<sup>+</sup> solutes, and x is the location in the astrocyte. Eq. S1 was discretized as follows using the second-order Crank-Nicolson method,

$$\frac{c^{n+1} - c^n}{\Delta t} = \frac{1}{2} \left[ \frac{dD^{n+1}}{dx} \frac{dc^{n+1}}{dx} + D \frac{d^2c^{n+1}}{dx^2} + \frac{dD^n}{dx} \frac{dc^n}{dx} + D \frac{d^2c^n}{dx^2} \right] \quad (\text{S2})$$

$$c^{n+1} - \frac{\Delta t}{2} \left[ \frac{dD^{n+1}}{dx} \frac{dc^{n+1}}{dx} + D \frac{d^2c^{n+1}}{dx^2} \right] = c^n + \frac{\Delta t}{2} \left[ \frac{dD^n}{dx} \frac{dc^n}{dx} + D \frac{d^2c^n}{dx^2} \right].$$

A nonuniform spatial discretization scheme for first and second derivative terms was used,

$$f'(x_i) = -\frac{h_{i+1}}{h_i H_i} f(x_{i-1}) + \frac{h_{i+1} - h_i}{h_i h_{i+1}} f(x_i) + \frac{h_i}{h_{i+1} H_i} f(x_{i+1})$$

$$f''(x_i) = \frac{2}{h_i H_i} f(x_{i-1}) - \frac{2}{h_i h_{i+1}} f(x_i) + \frac{2}{h_{i+1} H_i} f(x_{i+1}), \quad (\text{S3})$$

where  $H_i = h_i + h_{i+1}$ ,  $h_i = x_i - x_{i-1}$ . Finally, Eq. S1 was discretized as a tri-diagonal system (see last section of supplemental material for detailed procedure),

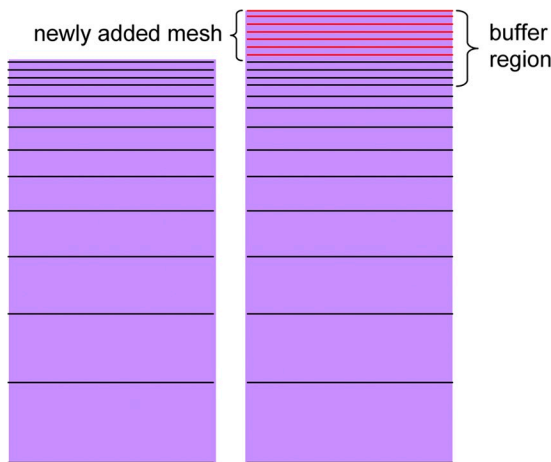


**Figure S1.** Schematic of buffer region and newly added mesh elements for computation of diffusion in astrocyte cytoplasm with a moving astrocyte–ECS boundary.

$$A_i c_{i-1} + B_i c_i + C_i c_{i+1} = RHS_i$$

$$A_i = -\frac{\Delta t}{2} \left[ f(D_i)^{n+1} \left( -\frac{h_{i+1}}{h_i H_i} \right)^{n+1} + \left( \frac{2}{h_i H_i} D_i \right)^{n+1} \right]$$

$$B_i = \left[ 1 - \frac{\Delta t}{2} \left( f(D_i)^{n+1} \left( \frac{h_{i+1} - h_i}{h_i h_{i+1}} \right)^{n+1} - \left( \frac{2}{h_i h_{i+1}} D_i \right)^{n+1} \right) \right]$$

$$C_i = -\frac{\Delta t}{2} \left[ f(D_i)^{n+1} \left( \frac{h_i}{h_{i+1} H_i} \right)^{n+1} + \left( \frac{2}{h_{i+1} H_i} D_i \right)^{n+1} \right]$$

$$RHS_i = \frac{\Delta t}{2} \left[ f(D_i)^{n+1} \left( -\frac{h_{i+1}}{h_i H_i} \right)^n + \left( \frac{2}{h_i H_i} D_i \right)^{n+1} \right] c_{i-1}$$

$$+ \left[ 1 + \frac{\Delta t}{2} \left( f(D_i)^{n+1} \left( \frac{h_{i+1} - h_i}{h_i h_{i+1}} \right)^{n+1} - \frac{\Delta t}{2} \left( \frac{2}{h_i h_{i+1}} D_i \right)^n \right) \right] c_i$$

$$+ \frac{\Delta t}{2} \left[ f(D_i)^{n+1} \left( \frac{h_i}{h_{i+1} H_i} \right)^{n+1} + \left( \frac{2}{h_{i+1} H_i} D_i \right)^{n+1} \right] c_{i+1}. \quad (\text{S4})$$

A moving-boundary computation was developed for the nonstationary astrocyte–ECS boundary, resulting from water flux. The computation used newly added mesh elements, requiring conservation of K<sup>+</sup> (and non-K<sup>+</sup>) solutes. After computation of water flux ( $J_v$ ) and the incremental astrocyte volume, new mesh elements at high density were added at the expanded boundary (Fig. S1). K<sup>+</sup> entering the astrocyte (from flux,  $J_K^a$ ) was added in a “buffer” (well-stirred) region as indicated.

$[K^+]_a$  and  $[\text{non-K}^+]_a$  in the buffer region were computed as,

$$[K^+]_a(t + \Delta t) = [K^+]_a(t) - \Delta t \cdot J_K^a / (\text{length of buffer region}) \quad (\text{S5})$$

$$[\text{non-K}^+]_a(t + \Delta t) = [\text{non-K}^+]_a(t), \quad (\text{S6})$$

where  $[K^+]_a(t) = 0$  and  $[\text{non-K}^+]_a(t) = 0$  in the newly added mesh elements and  $J_K^a$  has minus sign for K<sup>+</sup> flux from ECS to astrocyte.

The length of buffer region used in computations was 0.2  $\mu\text{m}$ . Fig. S2 shows astrocyte K<sup>+</sup> conservation in the computations, as well as little effect of buffer region length on  $[K^+]_e$ ,  $[K^+]_a$  buildup near the plasma membrane, and the kinetics of  $d_e$ .

After application of the flux boundary condition at the astrocyte membrane, diffusion inside the astrocyte was solved for a Neumann boundary condition (zero flux boundary condition) at the plasma membrane and at the opposite membrane.

#### Validation of solution of the diffusion equation

The numerical method for solution of the diffusion equation ( $u_t = Du_{xx}$ ), which was validated by comparison with the analytical solution for a step-function initial condition, is  $u(x, 0) = 0$  ( $x < 0$ ), 1 ( $x > 0$ ),

$$u(x, t) = 0.5(1 + \text{erf}[x / (4Dt)^{1/2}]). \quad (\text{S7})$$

Fig. S3 shows agreement between the analytical solution and numerical solution at different times ( $Dt = 0.1, 1, \text{ and } 10$ ).

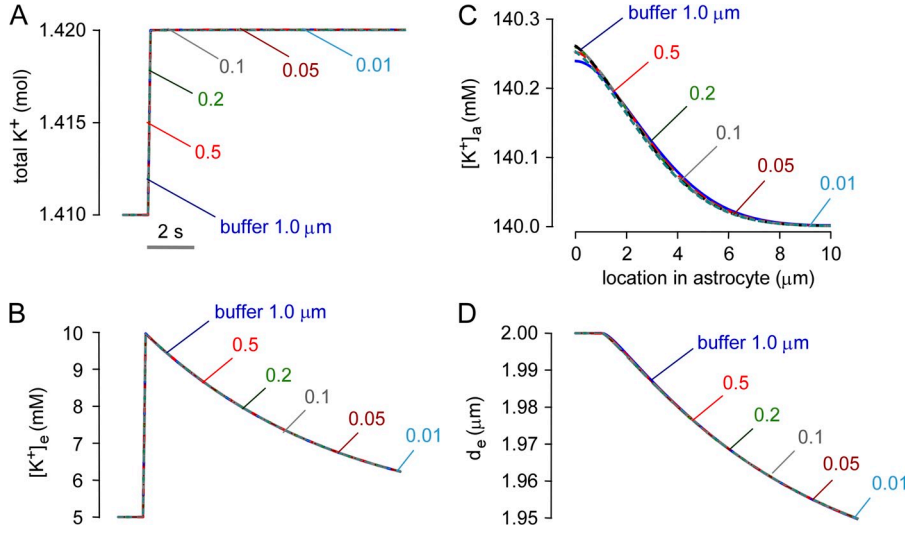


**Figure S2.** Examination of astrocyte K<sup>+</sup> concentration. (A) Conservation of total K<sup>+</sup> after neuroexcitation. Parameters:  $d_c = 2 \mu\text{m}$ ,  $P_K = 1.2 \times 10^{-5} \text{ cm/s}$ ,  $J_{K^+}^n = 10^{-8} \text{ mol/cm}^2/\text{s}$ , and  $P_f = 0.1 \text{ cm/s}$  for the indicated buffer region thickness. For the same parameter set, shown are time course of [K<sup>+</sup>]<sub>e</sub> (B), K<sup>+</sup> buildup in astrocyte cytoplasm (C), and d<sub>e</sub> (D).

### Alternative model variations

Alternative model variations were considered as shown schematically in Fig. S4. Fig. S5 shows computations done for indicated conditions for the well-mixed and diffusion-limited models (for  $D_a = 10^{-8} \text{ cm}^2/\text{s}$ ) for each condition, as compared with those for the standard model reported in the main text.

The first variation involved a large astrocyte volume ( $d_a = 100 \mu\text{m}$ ). There was little difference in computations from those with  $d_a = 10 \mu\text{m}$  (compare Fig. S5, A and B).

The second alternative variation of model involved nonuniform ECS geometry, with two thicknesses,  $d_{e1}$  and  $d_{e2}$ , with  $\alpha$  as the fraction with thickness  $d_{e1}$ .

Parameters were chosen as  $d_{e1} = 1 \mu\text{m}$ ,  $d_{e2} = 3 \mu\text{m}$ , and  $\alpha = 0.5$ . The ECS was considered to be a well-mixed region because of its small size and high diffusion coefficient ( $>10^{-6} \text{ cm}^2/\text{s}$ ). Because water and the K<sup>+</sup> flux are the same in regions 1 and 2, the new ECS volumes were calculated as

$$d_{e1}(t + \Delta t) = d_{e1}(t) + \Delta t \cdot J_V(t), \quad d_{e2}(t + \Delta t) = d_{e2}(t) + \Delta t \cdot J_V(t), \quad (\text{S8})$$

where  $J_V(t)$  is negative for water fluxes from ECS to astrocyte. [K<sup>+</sup>]<sub>de1</sub> and [K<sup>+</sup>]<sub>de2</sub> in the two regions in the ECS were calculated as,

$$\begin{aligned} [K^+]_{de1}(t + \Delta t) &= [K^+]_{de1}(t) d_{de1}(t) / d_{e1}(t + \Delta t) + \Delta t \cdot J_{K^+}^a / d_{de1}(t + \Delta t); \\ [K^+]_{de2}(t + \Delta t) &= [K^+]_{de2}(t) d_{de2}(t) / d_{e2}(t + \Delta t) + \Delta t \cdot J_{K^+}^a / d_{de2}(t + \Delta t). \end{aligned} \quad (\text{S9})$$

[K<sup>+</sup>]<sub>e</sub> was then taken as a weighted average in the well-mixed ECS,

$$[K^+]_e(t + \Delta t) = \{ [K^+]_{de1}(t + \Delta t) \cdot d_{e1}(t + \Delta t) + [K^+]_{de2}(t + \Delta t) \cdot d_{e2}(t + \Delta t) \} / \{ d_{e1}(t + \Delta t) + d_{e2}(t + \Delta t) \}. \quad (\text{S10})$$

Fig. S5 C shows that inclusion of a nonuniform ECS has little effect on model computations, because [K<sup>+</sup>]<sub>e</sub> is averaged in well-mixed ECS.

As a final alternative variation of model, electroneutral (membrane potential-independent) K<sup>+</sup> transport, corresponding to NKCC and KCC transporters, was considered. The activity of the K<sup>+</sup> pump, channel, and neutral transporter were  $J_{\text{pump}}$ ,  $\gamma J_{\text{pump}}$ ,

and  $(\gamma - 1)J_{\text{pump}}$ , respectively, to give zero K<sup>+</sup> flux before neuroexcitation. Electroneutral K<sup>+</sup> flux was described as follows, with activity  $(\gamma - 1)J_{\text{pump}}$  under resting conditions.

$$J_{\text{NT}} = (\gamma - 1)J_{\text{pump}} \{ \gamma_2 [K^+]_e(t) - [K^+]_a(t) \} / \{ \gamma_2 [K^+]_e(0) - [K^+]_a(0) \}. \quad (\text{S11})$$

Parameters were:  $\gamma = 3$ , to give relative activities of 1:3:2 by the K<sup>+</sup> pump, channel, and neutral transporter, respectively; and  $\gamma_2 = 3.4$  to give comparable conductive and electroneutral K<sup>+</sup> flux just after neuroexcitation. As shown in Fig. S6, the main conclusion, that there is little qualitative effect on computed results with inclusion of electroneutral transport, was robust and not affected by the exact choice of  $\gamma$ .

### Robustness of the K<sup>+</sup>/Cl<sup>-</sup> coupling ratio

In Eqs. 9–11 (Table 1), a factor of 2 was included to describe electroneutrality for conductive K<sup>+</sup> transport, implicitly assuming Cl<sup>-</sup> countertransport. This value is reasonable, though not rigorous, because both Na<sup>+</sup> and Cl<sup>-</sup> transport can occur. In Fig. S7, we performed computations to show that the major conclusions are robust and not dependent on the precise factor of 2 used, as factors of 1.5 and 3 gave qualitatively similar results.

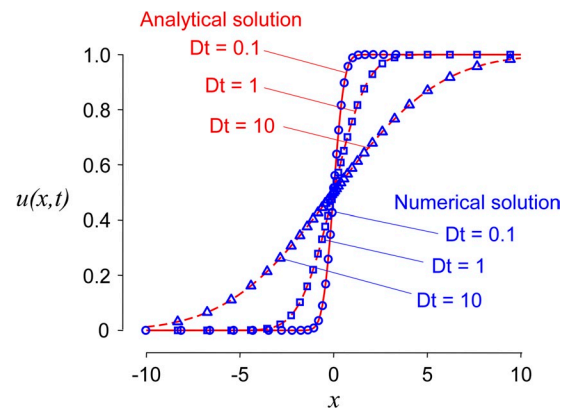


**Figure S3.** Agreement between numerical and analytical solutions to the diffusion equation for step-function initial condition.

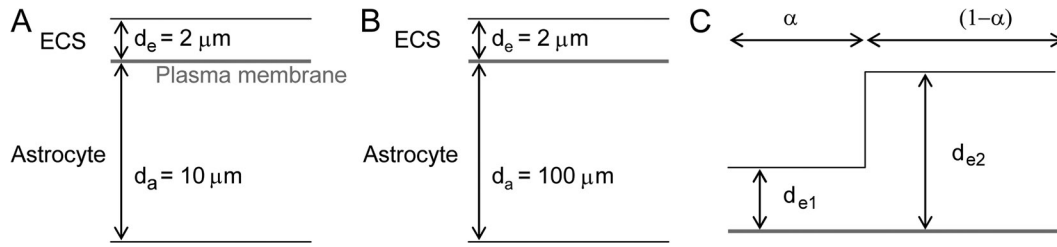


**Figure S4.** Schematic of model variations tested. (A) Standard model conditions. (B) Large astrocyte (thickness 100  $\mu\text{m}$ ). (C) Non-uniform ECS geometry.

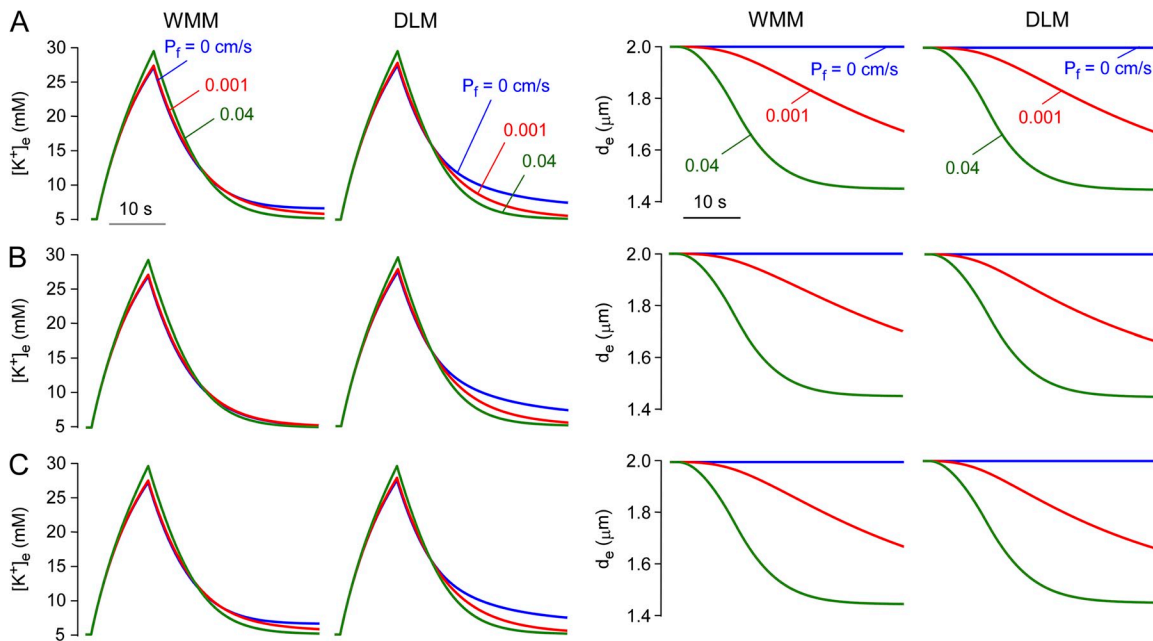


**Figure S5.** Predictions of alternative model variations. (A) Computations from Figs. 3 F and 5 C of the main text. (B) Expanded astrocyte cytoplasm modeled for  $d_a = 100 \mu\text{m}$ . Parameters:  $P_K = 1.3 \times 10^{-5} \text{ cm/s}$ ,  $J_{K^+o} = 8 \times 10^{-10} \text{ mol/cm}^2/\text{s}$ , and  $\Delta t_n = 10 \text{ s}$ , with the indicated  $P_f$ . (C) Non-uniform ECS thickness ( $d_c = 1$  and  $3 \mu\text{m}$ ), with  $P_K = 1.3 \times 10^{-5} \text{ cm/s}$ ,  $J_{K^+o} = 8 \times 10^{-10} \text{ mol/cm}^2/\text{s}$ , and  $\Delta t_n = 10 \text{ s}$ , with the indicated  $P_f$ . Parameter  $d_c$  is the mean of  $d_{c1}$  and  $d_{c2}$ .

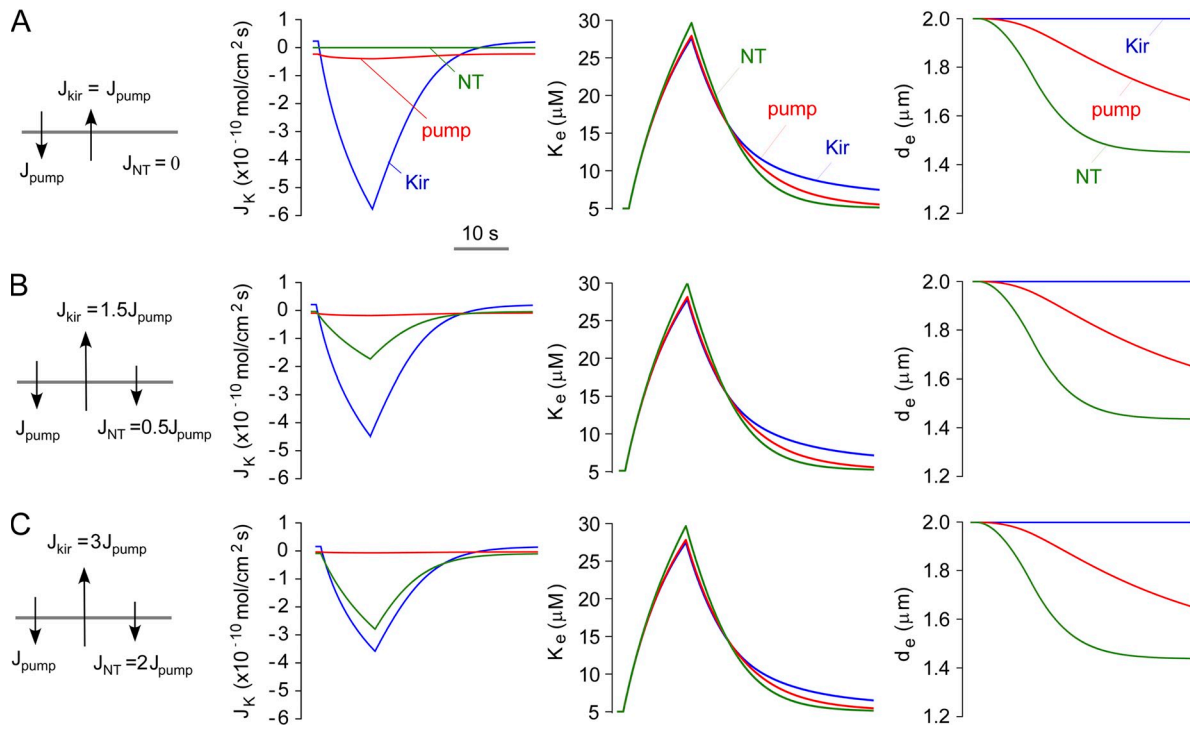


**Figure S6.** Inclusion of electroneutral (membrane potential-independent)  $K^+$  influx. (A)  $\gamma = 1$ . Parameters:  $P_K = 1.3 \times 10^{-7}$  cm/s,  $J_{K_o}^n = 8 \times 10^{-10}$  mol/cm<sup>2</sup>/s, and  $\Delta t_n = 10$  s (diffusion-limited model) with the indicated  $P_f$ . (B)  $\gamma = 1.5$ , with  $P_K = 6.7 \times 10^{-6}$  cm/s,  $J_{K_o}^n = 8 \times 10^{-10}$  mol/cm<sup>2</sup>/s, and  $\Delta t_n = 10$  s. (C)  $\gamma = 3.0$ , with  $P_K = 2.7 \times 10^{-6}$  cm/s,  $J_{K_o}^n = 8 \times 10^{-10}$  mol/cm<sup>2</sup>/s, and  $\Delta t_n = 10$  s.

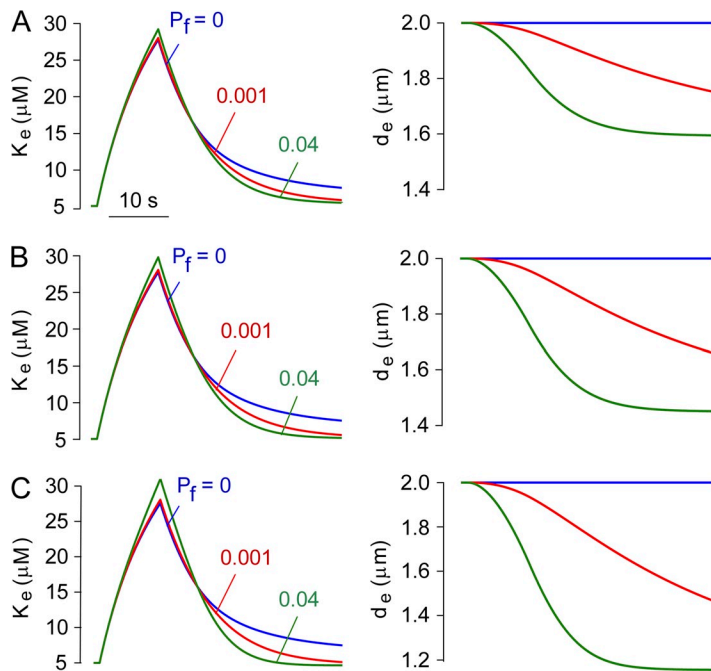


**Figure S7.** Predictions of alternative  $K^+/(Cl^-)$  coupling ratios of 1.5 (A), 2 (B) and 3 (C). Computations from Fig. 5 C. Parameters:  $P_K = 1.3 \times 10^{-5}$  cm/s,  $J_{K_o}^n = 8 \times 10^{-10}$  mol/cm<sup>2</sup>/s, and  $\Delta t_n = 10$  s, with the indicated  $P_f$ .

TABLE S1  
*Discretized equivalents of model differential and integration equations*

| Equation type  | Equation   | Equation number |
|--|--|-----------------|
| <b>Membrane potential equation</b>                   |  |                 |
| Membrane potential                                   | $\psi = (RT/F) \ln [(\alpha + [K^+]_e)/(\beta + [K^+]_a)]$   | 1               |
| <b>Flux equations</b>                                |  |                 |
| Potassium flux                                       | $J_{K^+} = P_K (\psi F/RT) ([K^+]_a - [K^+]_e \exp(-\psi F/RT)) / (1 - \exp(-\psi F/RT)) - J_{K^+ \text{ pump}}$ | 2               |
| Potassium pump flux                                  | $J_{K^+ \text{ pump}} = 2J_{K^+ \text{ pump}}(0) [1 + [K^+]_e(0)/(\Delta[K^+] - \Delta[K^+](0) - 2[K^+]_e(0))]$  | 3               |
| Water flux   | $J_v^a = P_f v_w (\Phi_e - \Phi_a)$  | 4               |
| <b>Equations for volume and concentration</b>        |  |                 |
| ECS volume   | $d_e(t + \Delta t) = d_e(t) + \Delta t J_v^a$  | 5               |
| Astrocyte volume                                     | $d_a(t + \Delta t) = d_a(t) - \Delta t J_v^a$  | 6               |
| [K <sup>+</sup> ] in the ECS                         | $[K^+]_e(t + \Delta t) = [K^+]_e(t) d_e(t)/d_e(t + \Delta t) + \Delta t \times J_{K^+}^a / d_e(t + \Delta t)$    | 7               |
| [K <sup>+</sup> ] in the astrocyte                   | $[K^+]_a(t + \Delta t) = [K^+]_a(t) d_a(t)/d_a(t + \Delta t) - \Delta t \times J_{K^+}^a / d_a(t + \Delta t)$    | 8               |
| <b>Equations for osmolarity</b>                      |  |                 |
| Osmolarity in the ECS                                | $\Phi_e(t + \Delta t) = \Phi_e(0) d_e(0)/d_e(t + \Delta t) + 2 \sum (\Delta t J_{K^+}^a) / d_e(t + \Delta t)$    | 9               |
| Osmolarity in the astrocyte                          | $\Phi_a(t + \Delta t) = \Phi_a(0) d_a(0)/d_a(t + \Delta t) - 2 \sum (\Delta t J_{K^+}^a) / d_a(t + \Delta t)$    | 10              |
| Non-K <sup>+</sup> osmolarity                        | $[\text{non-K}^+]_a = \Phi_a(t + \Delta t) - 2 [K^+]_a$  | 11              |
| <b>Diffusion equations</b>                           |  |                 |
| K <sup>+</sup> diffusion                             | $\partial [K^+] / \partial t = D_a \partial^2 [K^+] / \partial x^2$  | 12              |
| Non-K <sup>+</sup> diffusion                         | $\partial [\text{non-K}^+] / \partial t = D_a \partial^2 [\text{non-K}^+] / \partial x^2$                        | 13              |
| <b>Equation for flux through the moving membrane</b> |  |                 |
| Flux boundary condition                              | $\partial [K^+]_a / \partial t = -J_{K^+}^a / \delta$  | 14              |

Discretization equations for numerical solution of diffusion equations

$$\begin{aligned}
\frac{dc}{dt} &= \frac{d}{dx} \left( D \frac{dc}{dx} \right) = \frac{dD}{dx} \frac{dc}{dx} + D \frac{d^2c}{dx^2} \\
\frac{c^{n+1} - c^n}{\Delta t} &= \frac{1}{2} \left[ \frac{dD^{n+1}}{dx} \frac{dc^{n+1}}{dx} + D \frac{d^2c^{n+1}}{dx^2} + \frac{dD^n}{dx} \frac{dc^n}{dx} + D \frac{d^2c^n}{dx^2} \right] \\
c^{n+1} - \frac{\Delta t}{2} \left[ \frac{dD^{n+1}}{dx} \frac{dc^{n+1}}{dx} + D \frac{d^2c^{n+1}}{dx^2} \right] &= c^n + \frac{\Delta t}{2} \left[ \frac{dD^n}{dx} \frac{dc^n}{dx} + D \frac{d^2c^n}{dx^2} \right] \\
c^{n+1}_i - \frac{\Delta t}{2} \left[ \frac{dD^{n+1}}{dx} \frac{dc^{n+1}}{dx} + D \frac{d^2c^{n+1}}{dx^2} \right]_i &= c^n_i + \frac{\Delta t}{2} \left[ \frac{dD^n}{dx} \frac{dc^n}{dx} + D \frac{d^2c^n}{dx^2} \right]_i \\
c^{n+1}_i - \frac{\Delta t}{2} \left[ \left( -\frac{h_{i+1}}{h_i H_i} D_{i-1} + \frac{h_{i+1} - h_i}{h_i h_{i+1}} D_i + \frac{h_i}{h_{i+1} H_i} D_{i+1} \right) \left( -\frac{h_{i+1}}{h_i H_i} c_{i-1} + \frac{h_{i+1} - h_i}{h_i h_{i+1}} c_i + \frac{h_i}{h_{i+1} H_i} c_{i+1} \right) \right]^{n+1} \\
&- \frac{\Delta t}{2} \left[ \frac{2}{h_i H_i} D_i c_{i-1} - \frac{2}{h_i h_{i+1}} D_i c_i + \frac{2}{h_{i+1} H_i} D_i c_{i+1} \right]^{n+1} \\
&= c^n_i + \frac{\Delta t}{2} \left[ \left( -\frac{h_{i+1}}{h_i H_i} D_{i-1} + \frac{h_{i+1} - h_i}{h_i h_{i+1}} D_i + \frac{h_i}{h_{i+1} H_i} D_{i+1} \right) \left( -\frac{h_{i+1}}{h_i H_i} c_{i-1} + \frac{h_{i+1} - h_i}{h_i h_{i+1}} c_i + \frac{h_i}{h_{i+1} H_i} c_{i+1} \right) \right]^n \\
&+ \frac{\Delta t}{2} \left[ \frac{2}{h_i H_i} D_i c_{i-1} - \frac{2}{h_i h_{i+1}} D_i c_i + \frac{2}{h_{i+1} H_i} D_i c_{i+1} \right]^n \\
f(D_i) &= \left( -\frac{h_{i+1}}{h_i H_i} D_{i-1} + \frac{h_{i+1} - h_i}{h_i h_{i+1}} D_i + \frac{h_i}{h_{i+1} H_i} D_{i+1} \right) \\
c^{n+1}_i - \frac{\Delta t}{2} \left[ f(D_i)^{n+1} \left( -\frac{h_{i+1}}{h_i H_i} c_{i-1} + \frac{h_{i+1} - h_i}{h_i h_{i+1}} c_i + \frac{h_i}{h_{i+1} H_i} c_{i+1} \right)^{n+1} \right] &- \frac{\Delta t}{2} \left[ \frac{2}{h_i H_i} D_i c_{i-1} - \frac{2}{h_i h_{i+1}} D_i c_i + \frac{2}{h_{i+1} H_i} D_i c_{i+1} \right]^{n+1} \\
&= c^n_i + \frac{\Delta t}{2} \left[ f(D_i)^n \left( -\frac{h_{i+1}}{h_i H_i} c_{i-1} + \frac{h_{i+1} - h_i}{h_i h_{i+1}} c_i + \frac{h_i}{h_{i+1} H_i} c_{i+1} \right)^n \right] + \frac{\Delta t}{2} \left[ \frac{2}{h_i H_i} D_i c_{i-1} - \frac{2}{h_i h_{i+1}} D_i c_i + \frac{2}{h_{i+1} H_i} D_i c_{i+1} \right]^n \\
f(D_i) &= \left( -\frac{h_{i+1}}{h_i H_i} D_{i-1} + \frac{h_{i+1} - h_i}{h_i h_{i+1}} D_i + \frac{h_i}{h_{i+1} H_i} D_{i+1} \right) \\
c^{n+1}_i - \frac{\Delta t}{2} \left[ f(D_i)^{n+1} \left( -\frac{h_{i+1}}{h_i H_i} c_{i-1} + \frac{h_{i+1} - h_i}{h_i h_{i+1}} c_i + \frac{h_i}{h_{i+1} H_i} c_{i+1} \right)^{n+1} \right] &- \frac{\Delta t}{2} \left[ \frac{2}{h_i H_i} D_i c_{i-1} - \frac{2}{h_i h_{i+1}} D_i c_i + \frac{2}{h_{i+1} H_i} D_i c_{i+1} \right]^{n+1} \\
&= c^n_i + \frac{\Delta t}{2} \left[ f(D_i)^n \left( -\frac{h_{i+1}}{h_i H_i} c_{i-1} + \frac{h_{i+1} - h_i}{h_i h_{i+1}} c_i + \frac{h_i}{h_{i+1} H_i} c_{i+1} \right)^n \right] + \frac{\Delta t}{2} \left[ \frac{2}{h_i H_i} D_i c_{i-1} - \frac{2}{h_i h_{i+1}} D_i c_i + \frac{2}{h_{i+1} H_i} D_i c_{i+1} \right]^n \\
&- \frac{\Delta t}{2} \left[ f(D_i)^{n+1} \left( -\frac{h_{i+1}}{h_i H_i} \right)^{n+1} + \left( \frac{2}{h_i H_i} D_i \right)^{n+1} \right] c_{i-1} + \left[ 1 - \frac{\Delta t}{2} \left( f(D_i)^{n+1} \left( \frac{h_{i+1} - h_i}{h_i h_{i+1}} \right)^{n+1} - \frac{\Delta t}{2} \left( \frac{2}{h_i h_{i+1}} D_i \right)^{n+1} \right) \right] c_i \\
&- \frac{\Delta t}{2} \left[ f(D_i)^{n+1} \left( \frac{h_i}{h_{i+1} H_i} \right)^{n+1} + \left( \frac{2}{h_{i+1} H_i} D_i \right)^{n+1} \right] c_{i+1} \\
&= \frac{\Delta t}{2} \left[ f(D_i)^{n+1} \left( -\frac{h_{i+1}}{h_i H_i} \right)^n + \left( \frac{2}{h_i H_i} D_i \right)^{n+1} \right] c_{i-1} + \left[ 1 + \frac{\Delta t}{2} \left( f(D_i)^{n+1} \left( \frac{h_{i+1} - h_i}{h_i h_{i+1}} \right)^{n+1} - \frac{\Delta t}{2} \left( \frac{2}{h_i h_{i+1}} D_i \right)^n \right) \right] c_i \\
&+ \frac{\Delta t}{2} \left[ f(D_i)^{n+1} \left( \frac{h_i}{h_{i+1} H_i} \right)^{n+1} + \left( \frac{2}{h_{i+1} H_i} D_i \right)^{n+1} \right] c_{i+1}
\end{aligned}$$

$$A_i c_{i-1} + B_i c_i + C_i c_{i+1} = RHS_i$$

$$A_i = -\frac{\Delta t}{2} \left[ f(D_i)^{n+1} \left( -\frac{h_{i+1}}{h_i H_i} \right)^{n+1} + \left( \frac{2}{h_i H_i} D_i \right)^{n+1} \right]$$

$$B_i = \left[ 1 - \frac{\Delta t}{2} \left( f(D_i)^{n+1} \left( \frac{h_{i+1} - h_i}{h_i h_{i+1}} \right)^{n+1} - \left( \frac{2}{h_i h_{i+1}} D_i \right)^{n+1} \right) \right]$$

$$C_i = -\frac{\Delta t}{2} \left[ f(D_i)^{n+1} \left( \frac{h_i}{h_{i+1} H_i} \right)^{n+1} + \left( \frac{2}{h_{i+1} H_i} D_i \right)^{n+1} \right]$$

$$RHS_i = \frac{\Delta t}{2} \left[ f(D_i)^{n+1} \left( -\frac{h_{i+1}}{h_i H_i} \right)^n + \left( \frac{2}{h_i H_i} D_i \right)^{n+1} \right] c_{i-1} + \left[ 1 + \frac{\Delta t}{2} \left( f(D_i)^{n+1} \left( \frac{h_{i+1} - h_i}{h_i h_{i+1}} \right)^{n+1} - \frac{\Delta t}{2} \left( \frac{2}{h_i h_{i+1}} D_i \right)^n \right) \right] c_i$$

$$+ \frac{\Delta t}{2} \left[ f(D_i)^{n+1} \left( \frac{h_i}{h_{i+1} H_i} \right)^{n+1} + \left( \frac{2}{h_{i+1} H_i} D_i \right)^{n+1} \right] c_{i+1}$$